Linear-Threshold Dynamics for the Study of Epileptic Events

Federico Celi[1], Ahmed Allibhoy[2], Fabio Pasqualetti[1], and Jorge Cortés[2]

Abstract— In this letter, we provide a detailed characterization of the equilibria and bifurcations of two-dimensional linear-threshold models. Using the input to the system as the bifurcation parameter, we characterize the location of the admissible equilibria, show that bifurcations can arise only when equilibria lie on the boundary of well-defined regions of the state space, and prove that (codimension-one) bifurcations can only be of three different types: persistent, non-smooth fold, and Hopf. We show how these bifurcations change the qualitative properties of the system trajectories, and how these behaviors resemble prototypical patterns of EEG activity observed before, during, and after seizure events in the human brain. Our findings suggest that low-dimensional linear threshold models can effectively be used to model, analyze, predict, and ultimately regulate the interactions of neuronal populations in the human brain.

I. INTRODUCTION

Epileptic seizures are characterized by an excessive and abnormal neuronal activity in the brain. Given the severity of this condition and its diffusion (10% of people worldwide experience at least one seizure episode in their lifetime), there has been a shared effort among different scientific communities to understand and fight this disease. Thanks to the wide availability of electroencephalogram (EEG) readings of healthy and epileptic brains, several mathematical models aiming at characterizing and describing these behaviors have been proposed. Despite the large variety of waveforms observed in EEG signals, most phenomena can be characterized by a small number of typical recurring waveforms [1].

Meso-to-macroscopic models reproduce the global activity of clusters of neurons through their firing rate, as opposed to reproducing the neuron's individual spiking as done in microscopic models. The former approach benefits from a lower-dimensional system of otherwise complex dynamics and is referred to as neural mass modeling [2]. In particular, linear threshold networks (LTNs) are commonly used in computational neuroscience to model various cognitive phenomena in the brain, see [3], [4] and references therein. In this paper we characterize the properties of equilibria and bifurcations of planar LTNs, and show how the qualitative behaviors induced by these bifurcations closely maps to the waveforms observed in EEG signals collected before, during, and after seizure events.

Related work. The idea of using dynamical models to interpret and understand epileptic events is not new. Prior work include the Jansen and Rit model [5], [6], the Epileptor [7], and the well known Wilson-Cowan model, with a sigmoidal activation function, in [8]–[11]. Other notable results can be found, for instance, in [2], [12]–[14] and the references therein. Differently from these studies, we consider LTNs, which follow a piecewise-smooth flow [15], [16] and have been used to model a variety of brain activities [3], [4]. LTNs are also amenable to analytical study, a feature that sets them apart from other frameworks.

From a technical perspective, we rely on the rich theory of bifurcations of dynamical systems, which is well developed for smooth vector fields, e.g., see [17]. While results also exist to characterize the bifurcations of piecewise-smooth vector fields [18]–[20], a comprehensive theory is still lacking. Our results contribute to the development of this field by providing a characterization of the bifurcations of LTNs.

Paper contribution. The contributions of this paper are two-fold. First, using the input to the system as bifurcation parameter, we give a detailed analysis of the bifurcations occurring in planar LTNs. We derive explicit conditions on the parameters of the model to draw a set of different bifurcation diagrams, and study the qualitatively different behaviors that emerge in their phase diagrams. Second, we associate the behaviors originating from these bifurcations to prototypical waveforms observed in EEG signals during epileptic activities. This creates an effective map to understand epileptic features from the underlying dynamics, and paves the way to designing remedial controls.

Notation. Throughout the paper we use $\mathbb{R}$, $\mathbb{R}_{\geq 0}$, and $\mathbb{R}_{\leq 0}$ to denote the set of reals, nonnegative reals and nonpositive reals, respectively. We use bold letters for vectors and matrices. The identity matrix is denoted by $\mathbf{I}$. Given a vector $\mathbf{x} \in \mathbb{R}^n$, we use x_i to refer to its ith component. For $x \in \mathbb{R}$ and $m \in \mathbb{R}_{\geq 0}$, $[x]_0^m = \min\{\max\{x,0\}, m\}$, which is the projection of x onto $[0,m]$. Similarly, when $\mathbf{x} \in \mathbb{R}^n$ and $\mathbf{m} \in \mathbb{R}_{\geq 0}^n$, $[\mathbf{x}]_\mathbf{0}^\mathbf{m} = [[x_1]_0^{m_1} \ldots [x_n]_0^{m_n}]^T$. The open ball in $\mathbb{R}^n$ with radius $\epsilon > 0$ centered at $\mathbf{x} \in \mathbb{R}^n$ is denoted by $B_\epsilon(\mathbf{x}) = \{\mathbf{y} \in \mathbb{R}^n \mid \|\mathbf{y} - \mathbf{x}\| < \epsilon\}$.

II. PROBLEM FORMULATION

We model the interactions between populations of neurons trough a dynamical network with a nonlinear activation function, cf. [21]. Let $\mathbf{x}$ be the vector where each component represents the firing rate of a population of neurons, and $\mathbf{W} \in \mathbb{R}^{n \times n}$ be the synaptic weight matrix. The firing rates evolve according to a linear threshold model:

$$\dot{\mathbf{x}} = -\mathbf{x}(t) + [\mathbf{W}\mathbf{x}(t) + \mathbf{u}(t)]_\mathbf{0}^\mathbf{m}, \quad \mathbf{0} \leq \mathbf{x}(0) \leq \mathbf{m}, \quad (1)$$

where $\mathbf{m} \in \mathbb{R}_{>0}^n \cup \{\infty\}^n$. The vector $\mathbf{u}$ represents an external input to the system, such as unmodeled background activity.
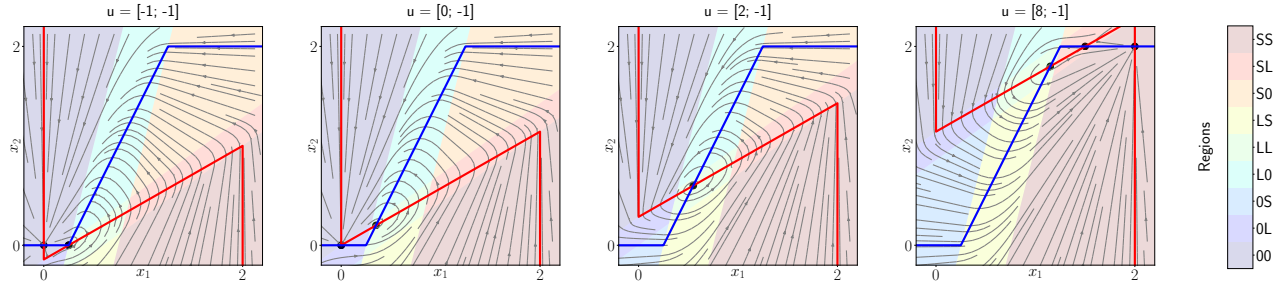
Fig. 1. Phase plot, regions of the state space, and nullclines for (2) with $W = [2, -2; 5, -2.5]$ and $\mathbf{m} = 2 \cdot \mathbf{1}_2$. By changing $\mathbf{u}$, the system exhibits different behaviors as equilibria may appear, disappear, and relocate in the state space. Higher (lower) values of u_1 (u_2) translate the x-nullcline N_1 in red (y-nullcline N_2 in blue) along the positive direction of x_2 (x_1).

Epilepsy is often described as an abrupt intermittent transition between highly ordered and disordered states [1]. In a dynamical systems' context, this may correspond to a qualitative change in the behavior of the system, which is typically linked to the study of bifurcations. Evidence suggests that, even during highly disruptive events such as seizures, the underlying connectivity structure between neurons does not experience a significant change in its nature, while the inputs to the system may be altered by exogenous and endogenous events. Following this evidence, here we study how changes in the input to (1) can generate qualitative changes in the behavior of the neurons firing rates.

We consider a network of excitatory and inhibitory neurons with all-to-all connectivity. Specifically, we focus on the dynamics in (1) with $n = 2$, where the state x_1 (x_2) is the lumped activity of the population of excitatory (inhibitory) neurons, which have positive (negative) feedforward contribution to the network. As our ensuing analysis reveals, the E-I pair case shows much of the complexity of the general case and is rich enough to capture a variety of epileptic behaviors. The dynamics of the E-I pair simplify to the following piecewise-smooth flow (PWSF):

$$\begin{bmatrix} \dot{x}_1 \\ \dot{x}_2 \end{bmatrix} = -\begin{bmatrix} x_1 \\ x_2 \end{bmatrix} + \left[\begin{bmatrix} a & -b \\ c & -d \end{bmatrix} \begin{bmatrix} x_1 \\ x_2 \end{bmatrix} + \begin{bmatrix} u_1 \\ u_2 \end{bmatrix} \right]_{\mathbf{0}}^{\mathbf{m}}. \quad (2)$$

We note that (2) resembles the classic Wilson-Cowan model [22] with, however, a piece-wise activation function in place of the more common sigmoidal function.

Throughout the paper, we use the notion of *nullclines* to characterize the equilibria of (1). In particular, the nullcline set $N_1 = \{x : \dot{x}_1 = 0\}$ is given by

$$x_1 = 0, \qquad\qquad x_2 \geq \frac{u_1}{b}, \quad (3a)$$

$$x_1 \in (0, m_1), \qquad x_2 = \frac{a-1}{b} x_1 + \frac{u_1}{b}, \quad (3b)$$

$$x_1 = m_1, \qquad x_2 \leq \frac{a-1}{b} m_1 + \frac{u_1}{b}. \quad (3c)$$

Similarly, the nullcline set $N_2 = \{x : \dot{x}_2 = 0\}$ is given by

$$x_1 \leq -\frac{u_2}{c}, \qquad\qquad x_2 = 0, \quad (4a)$$

$$x_1 = \frac{d+1}{c} x_2 - \frac{u_2}{c}, \qquad x_2 \in (0, m_2), \quad (4b)$$

$$x_1 \geq \frac{d+1}{c} m_2 - \frac{u_2}{c}, \qquad x_2 = m_2. \quad (4c)$$

Fig. 1 shows how changes in the input affect the nullclines on the plane and the resulting system behavior.

Beyond equilibria, limit cycles of (2) also play a key role in the system experiencing a rich repertoire of bifurcations and behaviors. The next result establishes conditions for their existence. The original statement appeared in [4], but here we provide a novel proof in Appendix A using the nullclines of (2), which is consistent with the rest of this work.

Theorem 2.1: (Limit cycles in E-I pairs [4]) All solutions to (2) (except the one originating from the unique unstable equilibrium in (6)) converge to a limit cycle if and only if

$$d + 2 < a, \quad (5a)$$

$$(a-1)(d+1) < bc, \quad (5b)$$

$$(a-1)m_1 < bm_2, \quad (5c)$$

$$0 < u_1 < bm_2 - (a-1)m_1, \quad (5d)$$

$$0 < (d+1)u_1 - bu_2 < [bc - (a-1)(d+1)]m_1. \quad (5e)$$

If (5) holds, the system has a unique unstable equilibrium:

$$\mathbf{x}^* = \frac{1}{bc - (1+d)(a-1)} \begin{bmatrix} (1+d)u_1 - bu_2 \\ cu_1 - (a-1)u_2 \end{bmatrix}. \quad (6)$$

III. BIFURCATION ANALYSIS

In this section we characterize the bifurcations of (2) as a function of the external input $\mathbf{u}$. We use this characterization in Section IV to explain empirical epileptic data. In what follows, we use the terminology and taxonomy of [18].

We begin by characterizing the system equilibria when the input $\mathbf{u}$ is fixed following [3]. The phase plane is partitioned into nine regions, parameterized by the parameter $\sigma \in \{0, \ell, s\}^2$, where the dynamics are affine. For each σ, the region is defined by

$$\Omega_\sigma = \{\mathbf{x} : (\mathbf{Wx} + \mathbf{u})_i \leq 0 \quad \text{if } \sigma_i = 0,$$
$$0 \leq (\mathbf{Wx} + \mathbf{u})_i \leq m_i \quad \text{if } \sigma_i = \ell,$$
$$(\mathbf{Wx} + \mathbf{u})_i \geq m_i \quad \text{if } \sigma_i = s\}.$$

Let Σ_σ^ℓ and Σ_σ^s be the diagonal matrices where $(\Sigma_\sigma^\ell)_{ii} = 1$ if $\sigma_i = \ell$, and $(\Sigma_\sigma^s)_{ii} = 1$ if $\sigma_i = s$. The dynamics can be written as $\dot{\mathbf{x}} = f_\sigma(\mathbf{x}, \mathbf{u})$ for $x \in \Omega_\sigma$, where

$$f_\sigma(\mathbf{x}, \mathbf{u}) = (-\mathbf{I} + \Sigma_\sigma^\ell \mathbf{W})\mathbf{x} + \Sigma_\sigma^\ell \mathbf{u} + \Sigma_\sigma^s \mathbf{m}.$$
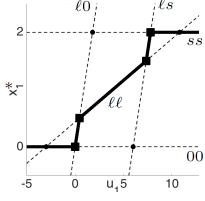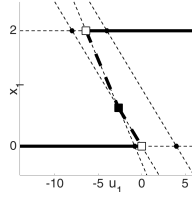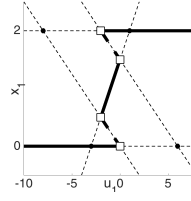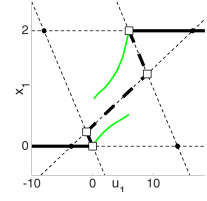
| (A) $a < 1$ | (B) $a > 1$ $(a-1)(d+1) > bc$ | (C) $a > 1$ $(a-1)(d+1) < bc$ $a < d+2$ | (D) $a > 1$ $(a-1)(d+1) < bc$ $a > d+2$ |

TABLE I

DIFFERENT TYPES OF BIFURCATION DIAGRAMS AS DISCUSSED IN THEOREM 3.1. THIN DASHED LINES SHOW FAMILIES OF VIRTUAL EQUILIBRIA. THICK LINES SHOW EQUILIBRIA: THICK SOLID LINES SHOW STABLE FIXED POINTS, WHILE THICK DASHED LINES SHOW UNSTABLE FIXED POINTS. BLACK (WHITE) SQUARE MARKERS SHOW P-BEB (NSF-BEB), WHILE CIRCLES SHOW NON-ADMISSIBLE BIFURCATION CANDIDATES. IN CASE (D) THE MAXIMUM AND MINIMUM VALUES OF THE LIMIT CYCLE ARE SHOWN IN COLOR.

Assumption 1: We assume that

(i) $\det(\mathbf{W}) \neq 0$,

(ii) $\det(-\mathbf{I} + \Sigma_\sigma^\ell \mathbf{W}) \neq 0$ for all $\sigma \in \{0, \ell, s\}^2$.

Note that this assumption is not restrictive since the set of matrices which fail to satisfy these conditions has zero Lebesgue measure. Under these assumptions, for each $\mathbf{u}$ there is a unique *equilibrium candidate* $\mathbf{x}_\sigma^*(\mathbf{u})$, such that $f_\sigma(\mathbf{x}_\sigma^*(\mathbf{u}), \mathbf{u}) = 0$. The equilibrium candidate $\mathbf{x}_\sigma^*$ is a smooth function of $\mathbf{u}$. When $\mathbf{x}_\sigma^*(\mathbf{u}) \in \Omega_\sigma$, we call the candidate *admissible* and $\mathbf{x}_\sigma^*(\mathbf{u})$ is an equilibrium of the system.

A bifurcation can occur only when $\mathbf{x}_\sigma^*(\mathbf{u})$ is on the boundary of Ω_σ. In this case, the equilibrium candidate $\mathbf{x}_\sigma^*$ overlaps with the equilibrium candidate of another region. This observation motivates the following definitions:

Definition 1: (Boundary equilibrium bifurcation (BEB)) We call $\mathbf{u}$ a *bifurcation candidate* if there exist distinct σ_1, σ_2 such that $\mathbf{x}_{\sigma_1}^*(\mathbf{u}) = \mathbf{x}_{\sigma_2}^*(\mathbf{u})$. A *boundary equilibrium bifurcation* occurs when $\mathbf{u}$ is a bifurcation candidate and $\mathbf{x}_\sigma^*$ is admissible in both Ω_{σ_1} and Ω_{σ_2}, i.e., when $\mathbf{x}_{\sigma_1}^*(\mathbf{u}) \in \Omega_{\sigma_1}$ and $\mathbf{x}_\sigma^*(\mathbf{u}) \in \Omega_{\sigma_2}$. □

Definition 2: (Types of BEBs) Suppose a boundary equilibrium bifurcation occurs at $\mathbf{u}$. Then, $\mathbf{u}$ is

(i) a *Persistent BEB* (P-BEB) if the number of equilibria is constant in a neighborhood of $\mathbf{u}$;

(ii) a *Non-smooth fold BEB* (NSF-BEB) if the number if equilibria is not constant in a neighborhood of $\mathbf{u}$;

(iii) a *Hopf bifurcation*[1] if it is an NSF-BEB such that a limit cycle emerges. □

We focus on codimension-one bifurcations, since they arise more frequently in biological systems than higher-dimensional bifurcations [12]. In particular, we choose u_1 as the bifurcation parameter, and leave u_2 constant. An equivalent analysis can be carried out using u_2 as the bifurcation parameter and keeping u_1 constant. We next state

[1] As highlighted in [18], the definition of Hopf bifurcation does not generalize well to PWSF since there is no sense in which eigenvalues cross the imaginary axis at the bifurcation onset. However, with a slight but common abuse of terminology, we refer to a Hopf bifurcation if the only attractor in the system is a limit cycle.

our main theoretical result (a proof is given in Appendix B), which characterizes explicitly the bifurcation diagram of (2). Because u_2 is constant, we abuse notation slightly by writing the equilibrium candidates as a function of u_1 only.

Theorem 3.1: (Bifurcation diagram) Let u_1 be the bifurcation parameter of the system (2), and let

$$- m_1 c < u_2 < (1 + d)m_2. \tag{7}$$

Then, there exist at most eight bifurcation candidates. Further, there exist four qualitatively different bifurcation diagrams induced by the following inequalities:

$$a < 1, \tag{8a}$$
$$(a - 1)(d + 1) < bc, \tag{8b}$$
$$a < d + 2, \tag{8c}$$

In particular, the possible bifurcation diagrams are defined as follows (see Table I for an illustration):

(A) If (8a) is satisfied, then there exists a unique equilibrium for every $\mathbf{u}$ and all bifurcations are P-BEB.

(B) If inequalities (8a) and (8b) are not satisfied, then the system has one equilibrium (for small and big values of u_1) or three equilibria. Then, bifurcations involving the $\Omega_{\ell\ell}$ region and only one other region are P-BEB. Otherwise, bifurcations are NSF-BEB.

(C) If (8b)-(8c) are satisfied and (8a) is not satisfied, then the bifurcation candidates involving either the region Ω_{00} or Ω_{ss} and only one other region are P-BEB. Otherwise, bifurcations are NSF-BEB.

(D) If (8b) is the only satisfied inequality, then the analysis of BEB is equivalent to that of Case C. However, condition (8c) makes $\mathbf{x}_{\ell\ell}^*$ an unstable fixed point resulting in a Hopf bifurcation at $\mathbf{u}_{00}^{\ell 0}$ and at $\mathbf{u}_{ss}^{\ell s}$.

Some comments are in order. First, the condition bounding u_2 limits the number of admissible equilibria to five (down from nine). For $u_2 < -m_1 c$, (resp. $u_2 > (1 + d)m_2$), we have $x_2 = 0$, (resp. $x_2 = m_2$), for all u_1, which are of little interest and we therefore exclude to keep the problem tractable. When (7) holds, the 5 equilibrium candidates are:

$$\mathbf{x}_{00}^*(u_1) = \mathbf{0}, \tag{9a}$$

Waveform Description	Dynamical Behavior	Clinical Setting
Normal background	Stable Fixed Point	Preictal activity
High-frequency Osc	Stable Limit Cycle	Interictal activity
Low-frequency Osc	Multistability	Interictal activity
Spikes	Multistability of $(0,0)$ and another fixed point	Seizure onset

TABLE II

EEG ACTIVITY AND FEATURES IN THE PHASE-SPACE [5].

$$\mathbf{x}_{\ell 0}^*(u_1) = \left(\frac{1}{1-a} u_1, 0 \right), \tag{9b}$$

$$\mathbf{x}_{\ell s}^*(u_1) = \left(\frac{1}{1-a} u_1 - \frac{b m_2}{1-a}, m_2 \right) \tag{9c}$$

$$\mathbf{x}_{\ell\ell}^*(u_1) = \left(\frac{(1+d)u_1 - b u_2}{(1+d)(1-a) + bc}, \frac{c u_1 + (1-a)u_2}{(1+d)(1-a) + bc} \right) \tag{9d}$$

$$\mathbf{x}_{ss}^*(u_1) = \mathbf{m}. \tag{9e}$$

We plot the five equilibria in (9) in Table I as a function of u_1 (thin-dashed lines). To make things easier to visualize, we only show the first coordinate of the equilibrium candidates. The first coordinate of (9a), which corresponds to the equilibrium candidate of the region Ω_{00}, is zero for every value of u_1 and is referenced as 00 in Case A of Table I. Similarly, the first coordinate of the equilibrium candidate (9d), which corresponds to the equilibrium candidate of the region $\Omega_{\ell\ell}$, varies linearly as a function of u_1 and is referenced as $\ell\ell$ in Case A of Table I. A bifurcation candidate arises whenever two of these lines intersect. Bifurcation candidates are shown as black dots in Table I. When the equilibrium candidates are admissible, then a BEB occurs, which is shown with a square in Table I. Further, when the number of equilibria remains constant on both sides of a bifurcation, a P-BEB occurs: this can be seen, for instance, in Case A, where all bifurcations are P-BEB (black squares). On the other hand, in Case B, the number of admissible equilibria to the left of the bifurcation occurring at $u_1 = 0$ are three ($\mathbf{x}_{00}^*$, $\mathbf{x}_{\ell 0}^*$ and $\mathbf{x}_{ss}^*$), while there is just one admissible equilibrium ($\mathbf{x}_{ss}^*$) to its right. This is an example of NSF-BEB, which is denoted with white squares.

IV. REPRODUCING EPILEPTIC PATTERNS

Here, we apply the results from Section III to show how linear threshold pairs can be used to model epileptic seizures. To obtain EEG-like waveforms from the linear threshold model, we simulate the dynamics in (2) by adding noise $\mathbf{w}$ in the linear threshold function:

$$\dot{\mathbf{x}} = -\mathbf{x} + [\mathbf{W}\mathbf{x} + \mathbf{u} + \mathbf{w}]_{\mathbf{0}}^{\mathbf{m}}.$$

The noise $\mathbf{w}$ is obtained by filtering Gaussian white-noise, with variance 1.4, through a filter with 1Hz cut-off frequency.

Although EEG measurements of the epileptic brain can exhibit a variety of behaviors, the EEG response can typically be constructed from a small number of prototypical waveforms [1]. The transition from healthy activity to a seizure is marked by a sudden dramatic change in the qualitative nature of the EEG signal. A seizure may contain several further changes before normal neurological activity is restored [23]. For example, the EEG recording of the seizure in Fig. 2

System	Bifurcations	Seizure behavior
A	P-BEB	
	P-BEB	No change
	P-BEB	
	P-BEB	
B	NSF	Normal → Spikes
	P-BEB	No change
	NSF	Spikes → Normal
C	NSF	Normal → Spikes
	NSF	Spikes → Normal
D	NSF	Normal → Spikes
	Hopf	Spikes → High frequency Oscillations
	Hopf	High Frequency Oscillations → Slow waves
	NSF	Slow waves → Normal

TABLE III

RELATIONSHIP BETWEEN ALL BIFURCATIONS EACH SYSTEM EXHIBITS (CF. DEFINITION 2 AND THEOREM 3.1), AND TRANSITION IN TYPE OF EEG ACTIVITY AS OUTLINED IN TABLE II.

.

can be divided into four segments based on the qualitative nature of the waveform, labeled S1, S2, S3, and S4. The healthy background activity, S1, is characterized by small fluctuations about a steady state. The presence of spikes in S2 indicates the onset of a seizure, with irregular low-frequency oscillations in S3, and quasi-sinusoidal oscillations in S4.

In [5], the authors introduce a "dictionary" relating prototypical waveforms to attractors of a nonlinear dynamical system. Here, we introduce a similar dictionary to associate prototypical waveforms to features in the phase-plane of the linear threshold model. This dictionary, along with the bifurcation analysis in Section III, can be used to systematically determine conditions on the connectivity matrix W so that the desired waveform can be replicated and the desired transitions can be obtained by varying the input to the excitatory and inhibitory populations.

In Table II, we relate the characteristic waveforms to features in the phase plane, and in Table III we use the bifurcation analysis from Section III to show which transitions between these waveforms each system is capable of exhibiting. These two tables can be used to explain epileptic patterns through the dynamical properties of linear-threshold pairs, to characterize possible seizures each pair can create, and to synthesize a system that can recreate an EEG pattern associated with a seizure event.

As we show next, with the correct values of parameters, the linear threshold model can have solutions sharing qualitative characteristics with EEG waveforms during epileptic seizures. In Fig. 3(a) we replicate the seizure in Fig. 2(b) having the characteristic waveforms S1-S4. Fig. 3(b) shows the input $u_1 + w_1$ as a function of time. To replicate the normal background activity in S1, we initialize system (D) choosing u_1 so that $(0,0)$ is the unique (stable) fixed point. The system then fluctuates around the equilibrium and there will be minimal activity in both the excitatory and inhibitory populations with sporadic firings caused by the system noise.

To obtain spikes in S2, we increase u_1 so that it is near the first NSF-BEB bifurcation. When $w_1 + u_1 < 0$, $\mathbf{x}_{00}$ is a stable fixed point. However, when $u_1 + w_1 > 0$, the system has a unique limit cycle and $\mathbf{x}_{00}$ is unstable. In this case,
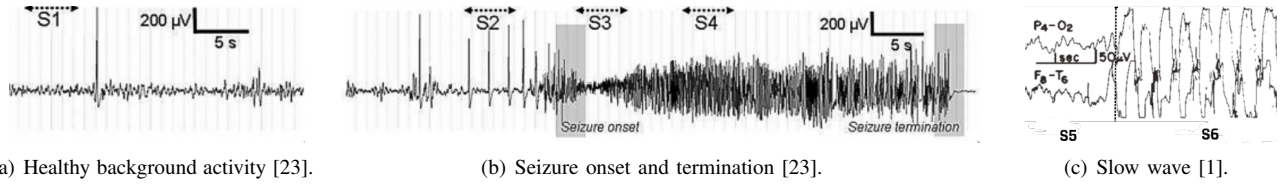
(a) Healthy background activity [23].

(b) Seizure onset and termination [23].

(c) Slow wave [1].

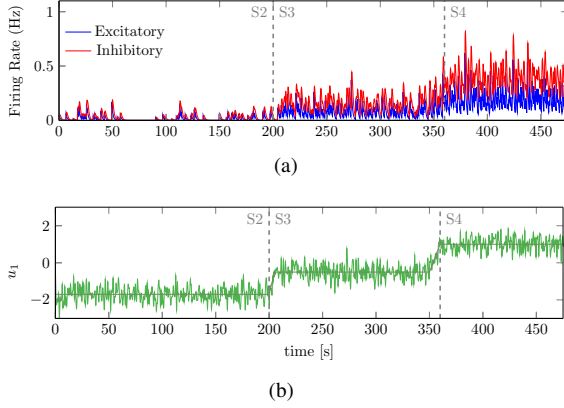Fig. 2. EEG recordings showing prototypical epileptic waveforms.

(a)

(b)

Fig. 3. Recreating epileptic dynamics using the LTN in Case D. Simulation of EEG recording (top) and input $u_1 + w_1$ as a function of time.
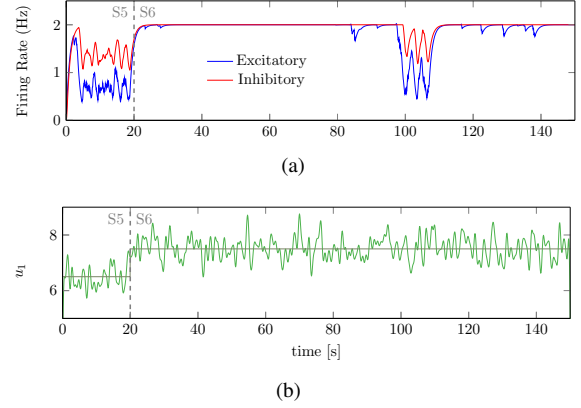

(a)

(b)

Fig. 4. Recreating slow waves using Case D. Simulation of EEG recording (top) and input $u_1 + w_1$ as a function of time.

the state $\mathbf{x}$ will initially oscillate until the noise restores the stability of $\mathbf{x}_{00}$, at which point the state will be attracted toward the origin. As u_1 is increased, the stable limit cycle persists even with noise. The state oscillates about $\mathbf{x}_{\ell\ell}$ with small amplitude as in S3. Increasing u_1 further increases both components of $\mathbf{x}_{\ell\ell}$ (see (9d)) as well as the amplitude of the oscillations, resulting in behavior similar to S4. We notice that, instead of increasing u_1, a similar behavior can be achieved by decreasing u_2 since it has a negative contribution on the value of $\mathbf{x}_{\ell\ell}^*$ in (9d). This is to be expected, since u_2 is the input to the inhibitory population. In fact, a higher input to a population translates in a higher firing rate for the population itself. This, in return, increases oscillations when increasing the input to an excitatory population, or decreases oscillations in the case of an inhibitory population.

An additional behavior typical of epileptic seizures is a slow wave, consisting of a low-frequency high amplitude oscillation with intermittent spikes. Fig. 2(c) shows an EEG recording of a seizure initially with high frequency oscillations in S5, then with slow waves with intermittent spikes in S6. To recreate slow waves in the linear threshold model, we initialize system (D) with u_1 near the second NSF-BEB bifurcation. When $w_1 > 0$, $\mathbf{x}_{ss}$ is a stable fixed point and system fluctuates around (m_1, m_2). When $w_1 < 0$, $\mathbf{x}_{ss}$ is unstable and the system has a limit cycle, resulting in a high frequency spiking which is halted once the stability of $\mathbf{x}_{ss}$ is restored. A simulation showing this behavior is in Fig. 4(a), with the corresponding input in Fig. 4(b)

V. Conclusions

We have shown how LTNs can be used to model a variety of prototypical brain waves measured in both healthy and epileptic brains. Focusing on a two-dimensional network, we provide an exhaustive analysis of the equilibria and bifurcations occurring as a function of the input to the system. We also provide a map and numerical evidence to associate these bifurcations to patterns of EEG signals observed before, during, and after seizure events. Directions of future research include a formal analysis of the results suggested in Section IV to relate the behavior of this model with real life EEG data, the study of higher-dimensional linear threshold models, and the design of control algorithms to detect and regulate seizure behaviors.

Appendix

A. Proof of Theorem 2.1

We first show how the conditions in the statement are necessary and sufficient for (2) to have a unique fixed point $\mathbf{x}^*$ which, furthermore, is unstable. For $\mathbf{x}^*$ to be the unique equilibrium, the nullclines N_1 and N_2 must intersect exactly once. This condition is satisfied when (i) the slope of the nullcline N_1 in the linear region is less than the ratio m_1/m_2, cf (5c); (ii) the slope of the nullcline N_1 is smaller than that of N_2 in the same region, cf. (5b); (iii) and $0 < \mathbf{x}_1(m_1) < m_2$, cf. (5d). Using the equations defining the nullclines, we obtain the coordinates of $\mathbf{x}^*$ in (6). Finally, since $\mathbf{x}^*$ needs to belong to the linear region, we have $0 < \mathbf{x}_1^* < m_1$, which reduces to (5e). Furthermore, the equilibrium is unstable since the Jacobian at this fixed point is $A = -I + W$ and, by (5a) and (5b), $\text{trace}(A)^2 - 4\det(A) < 0$. Thus, the eigenvalues of A are conjugate roots with real part $\frac{(-d-1)+(a-1)}{2} > 0$.

Next, let $\mathcal{R} = \{ \mathbf{x} \mid \mathbf{x} \in [0, m_1] \times [0, m_2] \setminus B_\epsilon(\mathbf{x}^*) \}$ for ϵ small enough so that $B_\epsilon(\mathbf{x}^*) \subset \Omega_{\ell\ell}$. Note that $\mathcal{R}$ is compact

by definition, and that $[0, m_1] \times [0, m_2]$ is forward invariant with respect to the dynamics (2). Furthermore, since $\mathbf{x}^*$ is the unique fixed point, is in the interior of the region $\Omega_{\ell\ell}$, and both eigenvalues of the Jacobian have a positive real component, we deduce that $\mathcal{R}$ is forward invariant. By the Poincaré-Bendixon Theorem [17, Chapter 7.3], since $\mathcal{R}$ is compact, forward invariant, and contains no fixed points, the system has a stable limit cycle in $\mathcal{R}$, concluding the proof. ∎

B. Proof of Theorem 3.1

Recall that $\mathbf{u}$ is a bifurcation candidate if and only if there exist distinct σ_1 and σ_2 such that $\mathbf{x}^*_{\sigma_1}(\mathbf{u}) = \mathbf{x}^*_{\sigma_2}(\mathbf{u})$. Examining only the x_1 component in equations (9a)-(9e), we see that these are affine in u_1. Moreover, the affine functions (9a) and (9e) are parallel and never intersect, so there is no bifurcation candidate when $\sigma_1 = 00$ and $\sigma_2 = ss$. By a similar line of reasoning, we conclude that there is no bifurcation candidate when $\sigma_1 = l0$ and $\sigma_2 = ls$. Hence there are only eight possible bifurcation candidates.

Let Ω_{σ_1} and Ω_{σ_2} be neighboring regions. Note that we can define h such that the dynamics (1), on $\Omega_{\sigma_1} \cup \Omega_{\sigma_2}$, become

$$\dot{x} = \begin{cases} f_{\sigma_1}(\mathbf{x}, u_1), & h(\mathbf{x}, u_1) \leq 0, \\ f_{\sigma_2}(\mathbf{x}, u_1), & h(\mathbf{x}, u_1) \geq 0, \end{cases} \quad (10)$$

where $h(\mathbf{x}, u_1) = 0$ on $\Omega_{\sigma_1} \cap \Omega_{\sigma_2}$. Let u_{σ_1, σ_2} be the bifurcation candidate, i.e., $\mathbf{x}^*_{\sigma_1}(u_{\sigma_1, \sigma_2}) = \mathbf{x}^*_{\sigma_2}(u_{\sigma_1, \sigma_2}) = \mathbf{x}^*$. Then, a BEB occurs if $h(\mathbf{x}^*, u_{\sigma_1, \sigma_2}) = 0$. Further, a P-BEB occurs if there exists a neighborhood of u_{σ_1, σ_2} such that, for all u_1 in such neighborhood, the following inequality holds:

$$h(\mathbf{x}^*_{\sigma_1}(u_1), u_1) h(\mathbf{x}^*_{\sigma_2}(u_1), u_1) > 0.$$

A NSF-BEB occurs instead when the inequality is not satisfied in any neighborhood of u_{σ_1, σ_2}.

We will now show explicitly how to compute the type of bifurcation when $\sigma_1 = 00$ and $\sigma_2 = \ell 0$. Let $\Omega_1 = \Omega_{00}$ and $\Omega_2 = \Omega_{\ell 0}$. Then, (10) becomes

$$\dot{x}_1 = \begin{cases} -x_1, & h(\mathbf{x}, u_1) < 0, \\ (a - 1)x_1 - bx_2 + u_1, & h(\mathbf{x}, u_1) > 0, \end{cases}$$

with $h(\mathbf{x}, u_1) = ax_1 - bx_2 + u_1$. From (9) we have $(x^*_{00}(u_1))_1 = 0$ and $(x^*_{\ell 0}(u_1))_1 = 1/(1 - a)u_1$. Hence, $h(\mathbf{x}^*_{00}(u_1), u_1) = u_1$ and $h(\mathbf{x}^*_{0\ell}(u_1), u_1) = u_1/(1 - a)$, which identifies a P-BEB at $u_1 = 0$ if and only if $a < 1$. This result is confirmed in Table I: in Case A, i.e., for $a < 1$, the bifurcation candidate involving regions Ω_{00} and $\Omega_{\ell 0}$ is a P-BEB, while it is a NSF-BEB in cases B, C, and D. An equivalent analysis involving the remaining seven bifurcation candidates can be performed, leading to the conditions of the theorem and the four scenarios highlighted in Table I. In the interest of space, the explicit computations are here omitted.

Finally, cases C and D exhibit equivalent conditions for the boundary equilibrium bifurcations. However, when condition (8c) is met, the equilibrium in $\Omega_{\ell\ell}$ is unstable (both eigenvalues of the $\mathbf{I} - \mathbf{W}$ are positive), and a limit cycle arises when the conditions in Theorem 2.1 are are also satisfied. This gives rise to a discontinuity-induced Hopf bifurcation, which differentiates case D from case C. ∎

References

[1] E. Niedermeyer and F. L. da Silva, *Electroencephalography: Basic Principles, Clinical Applications, and Related Fields*. Lippincott Williams & Wilkins, 2005.

[2] S. Coombes and Á. Byrne, *Next Generation Neural Mass Models*, pp. 1–16. Cham: Springer International Publishing, 2019.

[3] E. Nozari and J. Cortés, "Hierarchical selective recruitment in linear-threshold brain networks - Part I: Single-layer dynamics and selective inhibition," *IEEE Transactions on Automatic Control*, 2020.

[4] E. Nozari and J. Cortés, "Oscillations and coupling in interconnections of two-dimensional brain networks," in *American Control Conference*, pp. 193–198, 2019.

[5] J. Touboul, F. Wendling, P. Chauvel, and O. Faugeras, "Neural mass activity, bifurcations, and epilepsy," *Neural Computation*, vol. 23, no. 12, pp. 3232–3286, 2011.

[6] F. Grimbert and O. Faugeras, "Bifurcation analysis of jansen's neural mass model," *Neural Computation*, vol. 18, no. 12, pp. 3052–3068, 2006.

[7] V. K. Jirsa, W. C. Stacey, P. P. Quilichini, A. I. Ivanov, and C. Bernard, "On the nature of seizure dynamics," *Brain*, vol. 137, pp. 2210–2230, 06 2014.

[8] R. M. Borisyuk and A. B. Kirillov, "Bifurcation analysis of a neural network model," *Biological Cybernetics*, vol. 66, no. 4, pp. 319–325, 1992.

[9] Y. Wang, M. Goodfellow, P. N. Taylor, and G. Baier, "Phase space approach for modeling of epileptic dynamics," *Physical Review E - Statistical, Nonlinear, and Soft Matter Physics*, vol. 85, no. 6, pp. 1–11, 2012.

[10] H. G. Meijer, T. L. Eissa, B. Kiewiet, J. F. Neuman, C. A. Schevon, R. G. Emerson, R. R. Goodman, G. M. McKhann, C. J. Marcuccilli, A. K. Tryba, J. D. Cowan, S. A. van Gils, and W. van Drongelen, "Modeling focal epileptic activity in the wilson–cowan model with depolarization block," *The Journal of Mathematical Neuroscience*, vol. 5, no. 1, pp. 1–17, 2015.

[11] S. Coombes, Y. M. Lai, M. Şayli, and R. Thul, "Networks of piecewise linear neural mass models," *European Journal of Applied Mathematics*, vol. 29, no. 5, pp. 869–890, 2018.

[12] E. M. Izhikevich, "Neural excitability, spiking and bursting," *International Journal of Bifurcation and Chaos*, vol. 10, no. 6, pp. 1171–1266, 2000.

[13] E. Brown, J. Moehlis, and P. Holmes, "On the phase reduction and response dynamics of neural oscillator populations," *Neural Computation*, vol. 16, no. 4, pp. 673–715, 2004.

[14] F. L. da Silva, W. Blanes, S. N. Kalitzin, J. Parra, P. Suffczynski, and D. N. Velis, "Epilepsies as dynamical diseases of brain systems: Basic models of the transition between normal and epileptic activity," *Epilepsia*, vol. 44, no. s12, pp. 72–83, 2003.

[15] M. Johansson and M. Johanssn, *Piecewise Linear Control Systems*. Berlin, Heidelberg: Springer-Verlag, 2003.

[16] H. Lin and P. J. Antsaklis, "Stability and stabilizability of switched linear systems: a survey of recent results," *IEEE Transactions on Automatic Control*, vol. 54, no. 2, pp. 308–322, 2009.

[17] S. Strogatz, *Nonlinear Dynamics And Chaos: With Applications To Physics, Biology, Chemistry, And Engineering (Studies in Nonlinearity)*. Westview Press, 2001.

[18] M. Bernardo, C. Budd, A. Champneys, and P. Kowalczyk, *Piecewise-smooth Dynamical Systems: Theory and Applications*. Applied Mathematical Sciences, Springer London, 2008.

[19] R. Leine and H. Nijmeijer, *Dynamics and Bifurcations of Non-Smooth Mechanical Systems*. Lecture Notes in Applied and Computational Mechanics, Springer Berlin Heidelberg, 2013.

[20] A. Colombo, M. Di Bernardo, S. J. Hogan, and M. R. Jeffrey, "Bifurcations of piecewise smooth flows: Perspectives, methodologies and open problems," *Physica D: Nonlinear Phenomena*, vol. 241, no. 22, pp. 1845–1860, 2012.

[21] P. Dayan and L. F. Abbott, *Theoretical Neuroscience: Computational and Mathematical Modeling of Neural Systems*. Computational Neuroscience, Cambridge, MA: MIT Press, 2001.

[22] H. R. Wilson and J. D. Cowan, "Excitatory and inhibitory interactions in localized populations of model neurons," *Biophysical Journal*, vol. 12, no. 1, pp. 1–24, 1972.

[23] P. Chauvel, "Stereoelectroencephalography," *Multimethodological Assessment of the Epileptic Forms*, vol. 270, 1996.